Multifractal analysis of photoinduced cooperative phenomena

2008 J. Phys.: Condens. Matter 20 025212

(http://iopscience.iop.org/0953-8984/20/2/025212)

IOP PUBLISHING JOURNAL OF PHYSICS: CONDENSED MATTER

J. Phys.: Condens. Matter **20** (2008) 025212 (5pp) doi:10.1088/0953-8984/20/02/025212

Multifractal analysis of photoinduced cooperative phenomena

Kunio Ishida[1] **and Keiichiro Nasu**[2]

[1] Corporate Research and Development Center, Toshiba Corporation, 1 Komukaitoshiba-cho, Saiwai-ku, Kawasaki 212-8582, Japan
[2] Solid State Theory Division, Institute of Materials Structure Science, KEK, Graduate University for Advanced Study and CREST JST, 1-1 Oho, Tsukuba, Ibaraki 305-0801, Japan

E-mail: ishida@arl.rdc.toshiba.co.jp

Received 14 May 2007, in final form 14 October 2007
Published 6 December 2007
Online at stacks.iop.org/JPhysCM/20/025212

Abstract
We study the multifractal properties of the geometrical patterns which appear in the initial processes of photoinduced structural change. Employing a model of localized electrons coupled with a single-phonon mode, we calculate the Lipschitz–Hölder exponent α and singularity spectrum $f(\alpha)$ on the distribution of excited electronic states and molecular distortion by using the box-counting method, and discuss the temporal behavior of photoinduced domains.

1. Introduction

Recently photoinduced cooperative phenomena have been studied extensively both theoretically and experimentally [1]. These phenomena essentially include many-body effects regarding structural, magnetic, or ferroelectric properties induced by the injection of photoexcited states [2–6], and they are considered to occur by a common mechanism. However, particularly regarding theoretical studies, we are currently at a primary stage of searching for a clue to establish a physical picture of the phenomena [7–12], which we should obtain prior to the quantitative discussion of material-dependent properties. From this viewpoint, it is important to find model systems which reveal the elementary processes of the photoinduced cooperativity, i.e. we require model systems which show the cooperatively driven change in electronic states and/or structural properties triggered by the injection of photoexcited states.

We have proposed a model of interacting molecules which is suitable for describing the initial nucleation processes in the photoinduced cooperative phenomena [9–12]. With this model we showed that the interplay of vibrational coupling and dipole–dipole interactions between molecules leads to the growth of excited-state domains accompanied by excitation energy transfer. To be more precise, we showed that excited molecules that are introduced to the material will induce electronic state conversion in the other molecules, and that the coherent motion of the molecular distortion is important for understanding the dynamics of these nucleation processes. In relation to the experimental results, we also showed that the domain growth dynamics is also affected by the interdomain interactions, and that the conversion rate is a power of the excitation intensity, as observed in experiments [3, 12]. We should note that, according to these results, photoinduced domains have a certain internal structure, i.e. domains are not composed of uniformly distorted molecules but some geometrical patterns are observed in them. Since this nanoscale structure appears as a result of nucleation processes, it is important to analyze the patterns to understand the initial dynamics of the photoinduced cooperative phenomena.

On the other hand, recent advances in laser technology have made it possible to generate arbitrarily designed optical pulses, and control of the quantum mechanical states of materials with those pulses has become one of the central interests of research into future device applications [13]. Since it has been pointed out that photoinduced cooperativity is present even with extremely weak excitation [2–4], we consider that the coherent control of the above-mentioned phenomena will be useful for realizing energy-efficient devices.

In this paper we study the geometrical properties of a photoinduced domain in the coherent regime. For this purpose we particularly focus on the population of the excited electronic state and molecular distortion, and perform multifractal analysis [14–16] on the geometrical patterns represented by these properties, which is potentially one

of the most efficient and powerful tools for characterizing complicated geometrical structures and for analyzing the microscopic properties of the wavefunction of photoinduced domains.

2. Model and method

2.1. Model of interacting molecules on a lattice

As a minimal model to describe the photoinduced cooperativity, we employ a model of molecules arrayed on a square lattice. Since the elementary processes of photoinduced nucleation are excitation energy transfer between individual molecules, we extract a skeleton model which describes the energy transfer process through intermolecular interactions. Furthermore, in the present paper, we focus on the photoinduced cooperativity accompanied by a structural change of the materials, and hence the electron–phonon interactions between molecules are particularly important to the nucleation processes. Since we are interested in insulators, the itinerancy of electrons is less important for describing the basic properties of the initial nucleation processes, and the excitation energy is primarily carried by phonons instead.

As shown in the previous studies [9–12], the dynamics of nonadiabatic transition is one of the most important features of the photoinduced nucleation processes. Although the bifurcation rate of wavefunctions has been studied extensively [17] following the original study by Landau [18] and Zener [19], we have pointed out that the full quantization of the relevant vibration mode of molecules is necessary for pursuing the time-dependent properties of the growing domains.

The above discussion leads us to assume that the model molecules are composed of a localized electron with two energy levels coupled with a single molecular vibration mode. We also assume that the diabatic potential surfaces with respect to the given electronic levels are assumed to cross each other and that the nonadiabaticity is taken into account via 'spin-flip' interaction between two electronic states. These assumptions are sound if we refer to the experimental results in organic polymers [3] and spin-crossover complex [4, 5], in which structural change is observed with the cooperative change of optical properties.

As for the intermolecular interaction, we take into account three types of intermolecular interactions described below:

(i) Vibrational coupling, which is the interaction between the vibration mode of different molecules. This is also responsible for the dispersion of the relevant phonon mode.

(ii) Coulomb interaction between excited molecules, which is derived from a dipole–dipole interaction induced by electronic excitation. The interaction strength is taken up to the first order of the molecular distortions.

(iii) Electron-vibrational coupling, which describes the distortion of molecules induced by the excited-state dipole in the adjacent molecules.

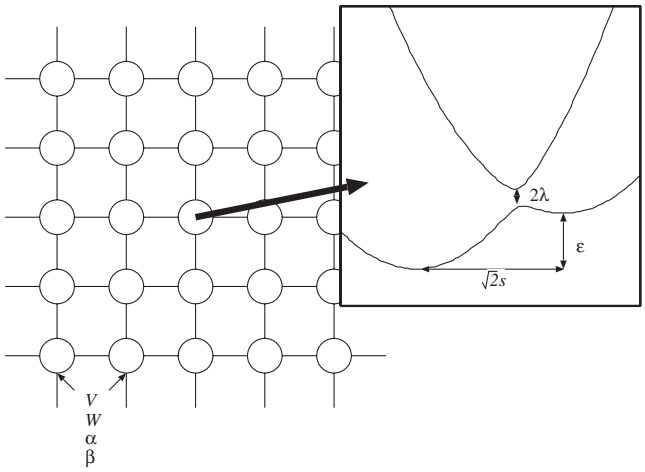

Figure 1. Schematic view of the model. Circles denote the molecules with two electronic states and a vibrational mode. Adiabatic potential energy surfaces for an individual molecule are shown in the inset.

Hence, the Hamiltonian in the present study is described by:

$$\begin{aligned}\mathcal{H} = \sum_{\vec{r}} \Bigg\{ & \frac{p_{\vec{r}}^2}{2} + \frac{\omega^2 u_{\vec{r}}^2}{2} + \Big(\sqrt{2\hbar\omega^3} s q_{\vec{r}} + \varepsilon\hbar\omega \\ & + s^2\hbar\omega\Big)\hat{n}_{\vec{r}} + \lambda\sigma_x^{\vec{r}} \Bigg\} \\ & + \sum_{\langle \vec{r},\vec{r}' \rangle} [\alpha\omega^2 (u_{\vec{r}} - \beta\hat{n}_{\vec{r}})(u_{\vec{r}'} - \beta\hat{n}_{\vec{r}'}) \\ & - \{V - W(u_{\vec{r}} + u_{\vec{r}'})\}\hat{n}_{\vec{r}}\hat{n}_{\vec{r}'}], \end{aligned} \tag{1}$$

where $p_{\vec{r}}$ and $u_{\vec{r}}$ are the quantized momentum and coordinate operators of the vibration mode at site $\vec{r}$, respectively. The second sum which gives the intermolecular interaction is taken over all the pairs on the nearest-neighbor sites. The electronic states at site $\vec{r}$ are denoted by $|\downarrow\rangle_{\vec{r}}$ (ground state) and $|\uparrow\rangle_{\vec{r}}$ (excited state), and $\sigma_i^{\vec{r}}$ $(i = x, y, z)$ are the Pauli matrices which act only on the electronic states of the molecule at site $\vec{r}$. A schematic view of the model is shown in figure 1.

In the present study we take $\hbar = \omega = 1$, and the unit of time is take to be $T = 2\pi/\hbar\omega$, which is equal to the vibrational period of a single molecule, which is typically $\sim$ 200 fs for organic molecules. As for the other parameters, we chose their values as $\varepsilon = 1.6$, $s = 1.4$, $V = 1.1$, $W = 0.2$, $\alpha = 0.1$, $\beta = 0.2$, and $\lambda = 0.2$. Although these values are typical for organic molecules for electron-vibration coupling [20] and the intermolecular Coulomb interaction [21], the values of the other parameters are not easy to determine, either from theoretical calculations or experimental results. We only mention that the order of magnitude for the parameters is estimated by referring to those for typical organic materials.

The quantized states on each diabatic energy surface of each molecule are the vibronic states of the molecule at site $\vec{r}$ described by $|n\sigma\rangle_{\vec{r}}$ $(n = 0, 1, 2, \ldots, \sigma = \uparrow, \downarrow)$ in the Fock representation [22, 23]. We note that this Ising-like model is similar to the one for studying the thermodynamical properties of the Jahn–Teller effect [24], although the nonequilibrium dynamics of the excited states in the model have not been understood.

We numerically solved the time-dependent Schrödinger equation for the Hamiltonian (1) on the 128 × 128 lattice,

$$\mathrm{i}\frac{\partial|\Phi(t)\rangle}{\partial t} = \mathcal{H}|\Phi(t)\rangle, \tag{2}$$

and obtained the photoinduced domain as a function of time. In these calculations we apply a mean-field approximation in order to deal with large system (up to 128 × 128 molecules), as in the previous studies [9–12].

2.2. Multifractal analysis of photoinduced domains

The photoinduced domain is obtained numerically by solving the time-dependent Schrödinger equation. Then the distribution of the excited-state population and/or molecular distortion is interpreted as geometrical patterns in two-dimensional space, and we performed a multifractal analysis [14–16] on them, which is used to reveal the scaling behavior of the domain. In this paper we discuss the geometrical patterns represented by the population of the excited electronic state defined by

$$N(\vec{r}, t) = \langle\Phi(t)|n_{\vec{r}}|\Phi(t)\rangle, \tag{3}$$

and the molecular distortion defined by

$$\zeta(\vec{r}, t) = \langle\Phi(t)|u_{\vec{r}}|\Phi(t)\rangle. \tag{4}$$

The multifractalicity of the patterns is characterized by the strength of the singularity obtained from the probability $\mu_i(\delta)$, the total count of $N(\vec{r}, t)$ or $\zeta^2(\vec{r}, t)$ in the i th box with edge length δ. Generally speaking, $\mu_i(\delta)$ is described by

$$\mu_i(\delta) = \delta^{\alpha}, \tag{5}$$

where α denotes the strength of the singularity, also known as the Lipschitz–Hölder exponent. When $\delta \to 0$, a different value of α corresponds to each point of the pattern. The probability of α lying between α' and $\alpha' + \mathrm{d}\alpha$ is

$$\rho(\alpha') \propto \delta^{-f(\alpha')}\,\mathrm{d}\alpha, \tag{6}$$

and thus $f(\alpha)$ corresponds to the fractal dimension of the set of small cells with a Lipschitz–Hölder exponent α.

The box-counting method [25–27] is often employed to obtain the α and $f(\alpha)$ in various systems [28–30]. This method is directly used to calculate the $(q-1)$th moment of $\mu_i(\delta)$ described by

$$Z_q = \sum_i \{\mu_i(\delta)\}^q \sim \delta^{\tau_q}. \tag{7}$$

α and $f(\alpha)$ are obtained by the Legendre transformation, i.e. the relation between $\alpha - f(\alpha)$ and $q - \tau_q$ is given by

$$\alpha(q) = \frac{\mathrm{d}\tau_q}{\mathrm{d}q} \tag{8}$$

$$f(\alpha(q)) = q\alpha - \tau_q. \tag{9}$$

We note that the $(q-1)$th moment emphasizes the concentrated region of the patterns for positive values of q, while it emphasizes the rarefied region for negative values of q.

3. Calculated results and discussion

The calculated results of the photoinduced domain for $t = 15$ are shown in figures 2(a) and (b). At $t = 0$ only a single molecule at the origin (center of the square) is in the Franck–Condon state, while the others are in the ground state. As the molecule at the origin distorts, electronic state conversion from $|\downarrow\rangle_{\vec{r}}$ to $|\uparrow\rangle_{\vec{r}}$ is induced and the excitation energy propagates in the system. As a result, the other molecules turn to be in the electronic excited state $|\uparrow\rangle_{\vec{r}'}$, and a domain-like structure gradually grows in the system (photoinduced nucleation processes). Although the vibronic state of such a domain holds the $D_{4\mathrm{h}}$ symmetry of the square lattice around the origin, we found that internal geometrical structure appears in the domain, as shown in the gradation of figures 2(a) and (b).

The Lipschitz–Hölder exponents α and the corresponding singularity spectra $f(\alpha)$ are calculated for $N(\vec{r}, t)$ and $\zeta^2(\vec{r}, t)$ and the results are shown in figures 3(a) and (b). In both figures, $f(\alpha)$ is convex and therefore shows the multifractal nature of the photoinduced domain. This multifractal nature is caused because the domain growth takes place in a hierarchical manner, i.e. electronic-state conversion occurs step by step around the initially excited molecule.

Since the minimum value of α ($\alpha_{\min}$) corresponds to the Lipschitz–Hölder exponent for $q \to \infty$, it represents the fractal properties of the most concentrated part of the domain, which is composed of totally converted molecules. Figures 3(a) and (b) show that $\alpha_{\min}$ for $N(\vec{r}, t)$ and $\zeta^2(\vec{r}, t)$ gives a consistent value of $\alpha_{\min}$ which increases as a function of time. The value of $f(\alpha_{\min})$ also increases from 0, reflecting the growth of the domain.

We stress that $f(\alpha_{\min})$ is less than 2, which means that the geometrical patterns in the domain shown in figure 2 has fractal geometry. Figures 3(a) and (b) also show that, as the domain grows, the variance of the patterns, in the sense of their multifractal nature, increases. These aspects are the quantitative description of the geometrical structure of the photoinduced domain shown in figure 2, and thus the multifractal analysis works well for understanding the patterns which appear in the domain.

The maximum value of α ($\alpha_{\max}$) shows the fractal properties of the most rarefied part of the domain. This part mostly describes the geometry of the unconverted molecules, i.e. the molecules outside the domain. We found that $\alpha_{\max}$ for both $N(\vec{r}, t)$ and $\zeta^2(\vec{r}, t)$ increases as a function of time. However, the value of $\alpha_{\max}$ for $\zeta^2(\vec{r}, t)$ changes prior to that for $N(\vec{r}, t)$. As a sound wave propagates in the system, molecular distortion is induced in the system and then population transfer takes place as a result. Thus, the oscillation of molecular distortion is reflected in the geometrical pattern earlier than the population transfer. We also mention that the variance of $\alpha_{\max}$ is affected by the system size, and that its absolute value should be discussed carefully.

It has been pointed out that a nanoscale fractal structure induces a change in the dynamics of chemical reactions, such as the reaction rate, by modifying the reaction field [31, 32]. The present results show that these chemical reactions can

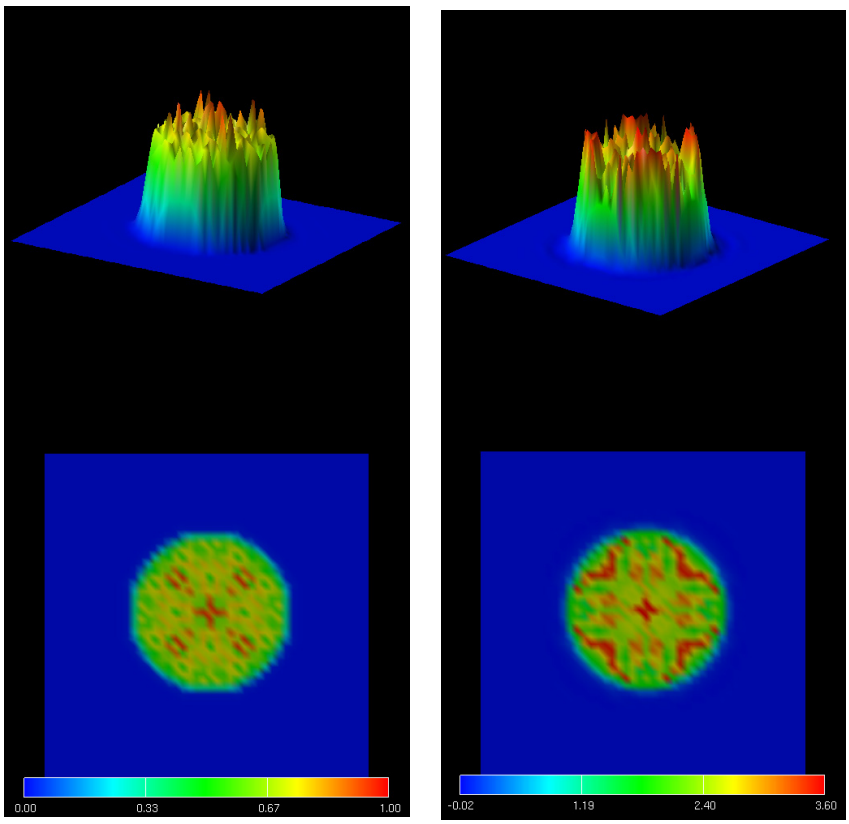

Figure 2. Photoinduced domain represented by population $N(\vec{r}, t)$ (left) and lattice distortion $\zeta(\vec{r}, t)$ (right) for $t = 15$. Only the 48×48 sites around the initially excited molecule are shown.

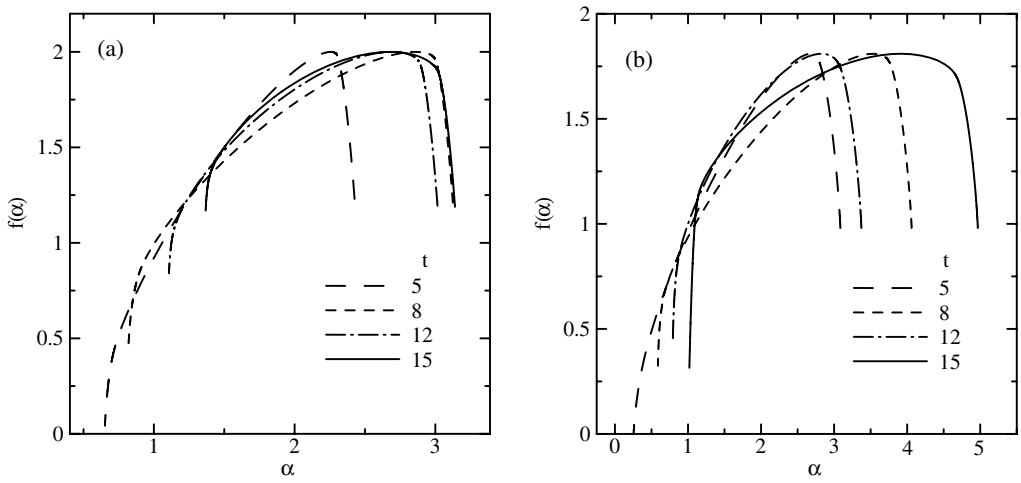

Figure 3. The $f(\alpha)$ curve for (a) $N(\vec{r}, t)$ and (b) $\zeta^2(\vec{r}, t)$ for $t = 5$, 8, 12, and 15.

be controlled by optical pulses, i.e. the reaction field can be modified if those materials in which photoinduced cooperative phenomena occur are placed around the reactant and/or catalyst. In particular, since the coherent dynamics of nucleation processes are important for understanding the domain structure [11], coherent control of photoinduced cooperative phenomena is very important for obtaining novel methods of chemical reaction control. Hence, we point out that, by making such composite materials, we can accelerate or decelerate chemical reactions by weak optical pulses due to the high efficiency of photoinduced cooperative phenomena [1].

We discuss the effect of decoherence on the multifractal patterns. As the vibrational coherence between molecules is lost, the phases of their vibrational coordinates differ from each other. As a result, the nanoscale structure in the photoinduced domain is blurred, and the contrast between the

patterns discussed in the present paper is reduced. Since, however, coherent phonons are observed typically for the first few picoseconds after photoexcitation [33], we point out that the present results are valid within the timescale discussed in the paper ($t \leqslant 15$), and that multifractal patterns are present in such a coherent regime. We stress that we aim to shed light on the effectiveness of the multifractal analysis of photoinduced domains, and that the present results show that we will have fruitful information from experimental results on the crystal structure and/or the electronic states. As for the experimental techniques for observing geometrical patterns in the coherent regime, we mention that time-resolved x-ray diffraction measurements will reveal the details of transient structure change. Since ultrashort pulse x-ray sources are under development [34, 35], multifractal analysis of the photoinduced domain will be available in the near future.

4. Conclusions

In this paper we have studied the multifractal nature of the photoinduced domain in molecular crystals. We found that, in the coherent regime, both the population of the excited state and the molecular distortion show a multifractal property characterized by the Lipschitz–Hölder exponent α and the singularity spectrum $f(\alpha)$. $\alpha_{\min}$ and $\alpha_{\max}$ are dependent on time after photoexcitation, and the dynamics of the pattern are understood by the variance of the $f(\alpha)$ curve for the growing domain. When these patterns are observed by time-resolved x-ray diffraction measurements, for example, we will obtain very important information on the coherent dynamics of photoinduced nucleation processes.

By realizing a nanoscale multifractal structure in real materials, we will be able to modify the reaction field by using appropriately designed optical pulses, and thus photoinduced cooperative phenomena will be a novel method for controlling chemical reactions. Since these patterns appear as a result of coherent dynamics of nucleation processes, coherent control of the initial dynamics of these phenomena is key to developing new such methods.

Acknowledgments

This work was supported by the Next Generation Super Computing Project, Nanoscience Program, Ministry of Education, Culture, Sports, Science and Technology, Japan, and the numerical calculations were carried out on computers at the Research Center for Computational Science, National Institutes of Natural Sciences, Japan.

References

[1] Nasu K (ed) 2004 *Photoinduced Phase Transitions* (Singapore: World Scientific)
[2] Koshihara S, Takahashi Y, Sakai H, Tokura Y and Luty T 1999 *J. Phys. Chem.* B **103** 2592
[3] Koshihara S, Tokura Y, Takeda K and Koda T 1995 *Phys. Rev.* B **52** 6265
[4] Mino A, Ogawa Y, Koshihara S, Urano C and Takagi H 1998 *Mol. Cryst. Liq. Cryst.* **314** 107
[5] Moussa N O, Molnár G, Bonhommeau S, Zwick A, Mouri S, Tanaka K, Real J A and Bousseksou A 2005 *Phys. Rev. Lett.* **94** 107205
[6] Costa J S, Guionneau P and Létard J F 2005 *J. Phys. Conf. Ser.* **21** 67
[7] Koshino K and Ogawa T 1998 *Phys. Rev.* B **58** 14804
[8] Mizouchi H and Nasu K 2000 *J. Phys. Soc. Japan* **69** 1543
[9] Ishida K and Nasu K 2005 *J. Phys. Conf. Ser.* **21** 118
[10] Ishida K 2006 *Phys. Status Solidi* c **3** 3438
[11] Ishida K and Nasu K 2007 *Phys. Rev.* B **76** 014302
[12] Ishida K and Nasu K 2007 Nonlinearity in the dynamics of photoinduced nucleation process *Preprint* cond-mat/07082869
[13] For a review, see Rice S A and Zhao M 2000 *Optical Control of Molecular Dynamics* (New York: Wiley)
[14] Halsey T, Jensen M, Kadanoff L, Procaccia I and Shraiman B 1986 *Phys. Rev.* A **33** 1141
[15] Paladin G and Vulpiani A 1987 *Phys. Rep.* C **156** 148
[16] Feder J 1988 *Fractals* (New York: Plenum)
[17] Zhu C and Nakamura H 1994 *J. Chem. Phys.* **101** 4855 and the references cited therein
[18] Landau L D 1932 *Phys. Zts. Sov.* **2** 46
[19] Zener C 1932 *Proc. R. Soc.* A **137** 696
[20] Horikoshi K, Misawa K, Lang R and Ishida K 2006 *Opt. Commun.* **259** 723
Horikoshi K, Misawa K and Lang R 2007 *J. Chem. Phys.* **127** 054104
[21] Salem L 1976 *Science* **191** 822
[22] Ishida K, Aiga F and Misawa K 2007 *J. Chem. Phys.* **127** 194304
[23] Cahill K E and Glauber R J 1969 *Phys. Rev.* **177** 1857
[24] Boukheddaden K 2004 *Prog. Theor. Phys.* **112** 205
[25] Meisel L V, Johnson M and Cote P J 1992 *Phys. Rev.* A **45** 6989
[26] Borgani S, Murante G, Provenzale A and Valdarinini R 1993 *Phys. Rev.* E **47** 3879
[27] Yamaguti M and Prado C P C 1997 *Phys. Rev.* E **55** 7726
[28] Stach S, Cybo J and Chmiela J 2001 *Mater. Charact.* **26** 163
[29] Kestener P and Arneodo A 2004 *Phys. Rev. Lett.* **93** 044501
[30] Chaudhari A, Yan C-C S and Lee S-L 2003 *J. Phys. A: Math. Gen.* **36** 3757
[31] de Gennes P G 1982 *J. Chem. Phys.* **76** 3316
[32] Gutfraind R, Sheintuch M and Avnir D 1991 *J. Chem. Phys.* **95** 6100
[33] Hasche T, Canzler T W, Scholz R, Hoffmann M, Schmidt K, Frauenheim Th and Leo K 2001 *Phys. Rev. Lett.* **86** 4060
[34] Goulielmakis E, Yakovlev V S, Cavalieri A L, Uiberacker M, Pervak V, Apolonski A, Kienberger R, Kleineberg U and Krausz F 2007 *Science* **317** 769
[35] Shintake T, Matsumoto H, Ishikawa T and Kitamura H 2001 *Proc. SPIE-Int. Soc. Opt. Eng.* **4500** 12